

ORIGINAL RESEARCH



## DOT1L affects colorectal carcinogenesis via altering T cell subsets and oncogenic pathway

Danfeng Sun<sup>a\*</sup>, Weichao Wang<sup>a\*</sup>, Fangfang Guo<sup>a</sup>, Michael R. Pitter<sup>a,b</sup>, Wan Du<sup>a</sup>, Shuang Wei<sup>a</sup>, Sara Grove<sup>a</sup>, Linda Vatan<sup>a</sup>, Yingxuan Chen<sup>a</sup>, Ilona Kryczek<sup>a</sup>, Eric R. Fearon<sup>a</sup>, Jing-Yuan Fang<sup>a</sup>, and Weiping Zou<sup>a,b</sup>

<sup>a</sup>Departments of Surgery, University of Michigan, Ann Arbor, Michigan, United States; <sup>b</sup>Division of Gastroenterology and Hepatology, Shanghai Jiao Tong University School of Medicine Affiliated Renji Hospital, Shanghai, China

### ABSTRACT

Chronic inflammation and oncogenic pathway activation are key-contributing factors in colorectal cancer pathogenesis. However, colorectal intrinsic mechanisms linking these two factors in cancer development are poorly defined. Here, we show that intestinal epithelial cell (IEC)-specific deletion of *Dot1l* histone methyltransferase (*Dot1l*<sup>ΔIEC</sup>) reduced H3K79 dimethylation (H3K79me2) in IECs and inhibited intestinal tumor formation in *Apc*<sup>Min</sup>- and AOM-DSS-induced colorectal cancer models. IEC-*Dot1l* abrogation was accompanied by alleviative colorectal inflammation and reduced Wnt/β-catenin signaling activation. Mechanistically, *Dot1l* deficiency resulted in an increase in Foxp3<sup>+</sup>RORγ<sup>+</sup> regulatory T (Treg) cells and a decrease in inflammatory Th17 and Th22 cells, thereby reducing local inflammation in the intestinal tumor microenvironment. Furthermore, *Dot1l* deficiency caused a reduction of H3K79me2 occupancies in the promoters of the Wnt/β-catenin signaling genes, thereby diminishing Wnt/β-catenin oncogenic signaling pathway activation in colorectal cancer cells. Clinically, high levels of tumor H3K79me2 were detected in patients with colorectal carcinomas as compared to adenomas, and negatively correlated with RORγ<sup>+</sup>FOXP3<sup>+</sup> Treg cells. Altogether, we conclude that DOT1L is an intrinsic molecular node connecting chronic immune activation and oncogenic signaling pathways in colorectal cancer. Our work suggests that targeting the DOT1L pathway may control colorectal carcinogenesis. **Significance:** IEC-intrinsic *DOT1L* controls T cell subset balance and key oncogenic pathway activation, impacting colorectal carcinogenesis.

### ARTICLE HISTORY

Received 25 August 2021  
Revised 10 March 2022  
Accepted 10 March 2022

### KEYWORDS



DOT1L; H3K79me2; colorectal cancer; regulatory T cell; FOXP3; RORγ; Th17 cell; Th22 cell

### Introduction


Colorectal cancer is one of the most common causes of cancer mortality in the United States and worldwide. Immune checkpoint therapy (ICB) has been approved to treat patients with unresectable or metastatic microsatellite instability-high (MSI-H) or mismatch repair deficient (dMMR) colorectal cancer.<sup>1,2</sup> Unfortunately, because few patients have these particular genetic alterations, a vast majority of patients with colorectal cancer are not responsive to ICB therapy, highlighting the critical need to unveil previously unknown cellular and molecular determinants of colorectal cancer etiology. Colorectal cancer development is mediated in part by accumulated somatic mutations in selected oncogenes and tumor suppressor genes.<sup>3–5</sup> The Wnt/β-catenin pathway regulates colorectal cancer cell proliferation, apoptosis, and contributes to colorectal carcinogenesis.<sup>6,7</sup> Histone acetyltransferase (HAT) proteins recruited by β-catenin/T cell factor (TCF) transcription factor complexes to selected target genes have been implicated in the activation of β-catenin/TCF target genes.<sup>8,9</sup> These findings highlight the likely important roles that chromatin modifications have in modulating the Wnt/β-catenin signaling pathway to regulate gene expression in colorectal carcinogenesis.

The disruptor of telomeric silencing 1-like (*DOT1L*) protein mediates histone 3 lysine 79 (H3K79) methylation.<sup>10</sup> *DOT1L* plays a role in mixed-lineage leukemia (MLL),<sup>11,12</sup> and T cell polyfunctionality and survival.<sup>13</sup> It has been elucidated that *DOT1L* is activated by Th22 cells in human colorectal cancer cells.<sup>14</sup> Furthermore, a DOT1L-containing complex has been linked to the Wnt signaling pathway in *Drosophila*<sup>15</sup> and zebrafish.<sup>16</sup> Thus, prior works suggest a potential role of *DOT1L* in colorectal carcinogenesis. To address this possibility, we pursued studies of intestinal epithelial cell (IEC)-intrinsic abrogation of *Dot1l* function in the Wnt/β-catenin pathway activation in mouse colorectal tumorigenesis.

On the other hand, chronic immune activation-associated inflammation has been implicated in colorectal cancer development.<sup>17,18</sup> However, whether there exists an intestinal intrinsic mechanism controlling the balance among gut T cell subsets, particularly inflammatory Th17 and Th22 cells, and RORγ<sup>+</sup>Foxp3<sup>+</sup> regulatory T cells, and affects colorectal cancer pathogenesis remains unknown. To answer this question, using mouse colorectal cancer models with IEC-specific deletion of *Dot1l* histone methyltransferase (*Dot1l*<sup>ΔIEC</sup>), we examined a potential impact of intestinal epithelial cell *DOT1L* on

**CONTACT** Weiping Zou  [wzou@med.umich.edu](mailto:wzou@med.umich.edu)  Departments of Surgery, University of Michigan, Ann Arbor, Michigan, United States

\*These authors contributed equally to this work.

 Supplemental data for this article can be accessed on the [publisher's website](#)

© 2022 The Author(s). Published with license by Taylor & Francis Group, LLC.

This is an Open Access article distributed under the terms of the Creative Commons Attribution-NonCommercial License (<http://creativecommons.org/licenses/by-nc/4.0/>), which permits unrestricted non-commercial use, distribution, and reproduction in any medium, provided the original work is properly cited.

immune cell subsets in the colorectal cancer microenvironment, and extended our studies to patients with colorectal adenoma and carcinoma.

In the work presented here, we demonstrate that intestinal *DOT1L*-mediated H3K79 methylation, as an intrinsic mechanism, controls both the Wnt/ $\beta$ -catenin activation and immune cell subset balance, thereby contributing to colorectal cancer development.

## Materials and methods

### Human subjects

Treatment-naïve patients with colorectal adenoma and early colorectal carcinoma were recruited for this study.<sup>19</sup> Human subjects were from Renji Hospital affiliated to Shanghai Jiaotong University School of Medicine between 2012 and 2017. Patients were pathologically and clinically diagnosed with colorectal adenoma or early colorectal cancer. Informed consent was obtained from the patients before sample collection in accordance with institutional guidelines. The Ethics Committees in the Renji Hospital approved the study protocol. Patient characteristics were detailed in the Supplementary Table S1.

### Mouse strains

*Dot1l<sup>FF</sup>* mice<sup>12</sup> were bred to C57BL/6 mice expressing Cre-recombinase under the control of the *Villin* promoter<sup>20</sup> to generate intestinal epithelial cell (IEC) specific *Dot1l* knockout (*Dot1l<sup>ΔIEC</sup>*) mice. Genotypes were determined by PCR. Age- and gender-matched mice were used for all experiments. *Apc<sup>Min</sup>* mice (C57BL/6 *J-Apc<sup>Min</sup>/J*; stock 002020, the Jackson Laboratory) were bred with *Dot1l<sup>FF</sup>*; *Vil-Cre* mice to generate *Apc<sup>Min</sup>*; *Vil-Cre*; *Dot1l<sup>FF</sup>* (*Dot1l<sup>ΔIEC</sup> Apc<sup>Min</sup>*) mice, and *Apc<sup>Min</sup>*; *Dot1l<sup>FF</sup>* (*Dot1l<sup>FF</sup> Apc<sup>Min</sup>*) control littermates. Mouse studies were approved by the Institutional Animal Care & Use Committee of the University of Michigan.

### Murine colorectal inflammation and tumor models

*Dot1l<sup>FF</sup>* and *Dot1l<sup>ΔIEC</sup>* littermate mice were injected intraperitoneally with 10 mg of azoxymethane (AOM) (Sigma) per kilogram body weight. Five days later, 1.8% Dextran sulfate sodium salt (DSS) (colitis grade (36,000–50,000) (MP Biomedicals) was given in drinking water for 5 days followed by regular drinking water for 16 days. This cycle was repeated twice, and mice were sacrificed on day 70 or at the indicated time. In colorectal inflammation model, mice were fed with 1.8% DSS water for 5 days and followed with regular water for 4 days. *Dot1l<sup>FF</sup> Apc<sup>Min</sup>* and *Dot1l<sup>ΔIEC</sup> Apc<sup>Min</sup>* littermates were maintained for 6–7 months to assess spontaneous colorectal cancer development or were given drinking water with 1.8% DSS for 5 days, followed by regular water for 30 days to assess colorectal cancer development.

### Colorectal tumor organoid culture

Colorectal tumor organoid cultures were performed as described previously<sup>21</sup> with minor modifications. Briefly, tumor tissues were mechanically separated from surrounding

normal tissues and washed in PBS containing 100 U/ml penicillin and 100  $\mu$ g/ml streptomycin. These antibiotics were added to all solutions used in the following procedure. After washing with PBS, tumor tissues were cut into small pieces and digested with 200 U/ml type IV collagenase for 2 hours. The digested tumor tissue was passed through a 70- $\mu$ m cell strainer. Then, 10000 tumor cells were mixed with Matrigel (Fisher Scientific) and seeded in a 24-well plate. 15 minutes after the Matrigel polymerization, DMEM/F12 medium (ThermoFisher Scientific) contains 1 $\times$  Glutamax (ThermoFisher Scientific), 1 M HEPES (Life Technologies), 1 $\times$  N2 supplement (ThermoFisher Scientific), 1 $\times$  B27 supplement (ThermoFisher Scientific), and 50 ng/ $\mu$ l epidermal growth factor (EGF; Sigma) was added to the plate.

### IEC harvest, real-time PCR, and Western blotting

IECs were isolated from murine samples by shaking intestinal tissue in 1 mM EDTA/1 mM DTT and 5% FCS at 37°C for 10 min, resulting in 80–90% EpCAM<sup>+</sup> IEC purity. RNA was isolated from cells using TRIzol (ThermoFisher Scientific) reagent then subjected to reverse transcription with AMV reverse transcriptase (Promega). Real-time PCR was performed using SYBR green chemistry (Applied Biosystems). Reactions were run on a real-time PCR system (StepOne Plus Real-Time PCR System; Applied Biosystems) Specific primers are listed in Supplementary Table S2. For Western blotting, IECs were lysed in a modified RIPA buffer (ThermoFisher Scientific) and lysates were subjected to immunoblot analysis. Blots were probed with rabbit anti-H3K79me2, H3K79me3, H3K4me2, H3K4me3, H3K27me3 (Abcam), total H3 (Cell Signaling), and GAPDH (Invitrogen).

### Human colorectal cancer cell culture and lentiviral transduction

Human colorectal cancer cell lines DLD-1 and HT29 were obtained from ATCC. Lentiviral vectors were used to transduce colorectal cancer cells and establish stable cell lines. The lentiviral transduction efficiency was confirmed by GFP which was co-expressed by the lentiviral vector. The knockdown efficiency was assessed by immunoblotting. The vectors included pGIPZ lentiviral vector encoding gene-specific shRNAs for *DOT1L* or scrambled shRNA (Puromycin resistant).<sup>14</sup> Specific primers are listed in Supplementary Table S2.

### RNA extraction and quantitative PCR

Total RNA was isolated from cells by column purification (Direct-zol RNA Miniprep Kit, Zymo Research) with DNase treatment. cDNA was generated using High-Capacity cDNA Reverse Transcription Kit (ThermoFisher Scientific). Quantitative PCR (qPCR) was performed on cDNA using Fast SYBR Green Master Mix (Thermo Fisher Scientific) on a StepOnePlus Real-Time PCR System (Thermo Fisher Scientific). Gene expression was quantified using the primers listed in Supplementary Table S2.

### Chromatin immunoprecipitation (ChIP) assay

ChIP assay was performed according to the protocol (Upstate, Millipore) as previously described.<sup>14,22</sup> Crosslinking was performed with 1% formaldehyde or 1% paraformaldehyde for 10 minutes. To enhance cell lysis, we ran the lysate through a 27 g needle three times and flash froze it in  $-80^{\circ}\text{C}$ . Sonication was then performed with the Misonix 4000 water bath sonication unit at 15% amplitude for 10 minutes. Protein/DNA complex was precipitated by specific antibodies against H3K79me2 (Abcam) and IgG control (Millipore). Then, DNA was purified using DNA Purification Kit (Qiagen). ChIP-enriched chromatin was used for Real-Time PCR, relative expression level is normalized to Input. Specific primers are listed in Supplementary Table S3.

### Flow cytometry

To isolate lamina propria immune cells, IEC and intraepithelial lymphocyte layers were first stripped by shaking sections of large intestine in 5 mM EDTA/1 mM DTT. Remaining tissue was digested with collagenase (0.5 mg/ml) to obtain single cell suspensions. For flow cytometry, cells were stained with a combination of the following fluorescence-conjugated monoclonal antibodies, anti-CD3 (clone: 500A2), anti-CD4 (clone: RM4-5), anti-Foxp3 (clone: FJK-16s), anti-CD45 (clone: 30-F11), anti-ROR $\gamma$ t (clone: Q21-559), anti-IL-17A (clone: TC11-18H10), and anti-IL-22 (clone: 1H8PWSR) (BD-Biosciences or Thermo-Fisher). Samples were acquired on an LSR II (BD Biosciences) and were analyzed with FACSDiva software (BD Biosciences).

### Histology, immunohistochemistry, and immunofluorescence

For bromodeoxyuridine (BrdU) staining, 200  $\mu\text{L}$  of BrdU Labeling Reagent (ThermoFisher Scientific) was injected into mouse peritoneal cavity. Mice were sacrificed 2 hours after BrdU injection. The same segment of distal colorectal was fixed in 10% neutral formalin and paraffin embedded. Proliferating cells were detected with BrdU detection kit (BD Bioscience). Tissues were counterstained with hematoxylin. The number of BrdU-positive cells was quantified by number of cells in intact well-orientated crypts.

Immunofluorescence staining in mouse tissues. Frozen mouse colorectal tissue sections were incubated with anti-mouse  $\beta$ -catenin (1:200, BD Biosciences) and anti-mouse Axin2 (1:200, Abcam), followed by Alexa Fluor 488- or Alexa Fluor 594-conjugated secondary antibodies (Life Technologies) and DAPI (1  $\mu\text{g}/\text{mL}$ , Sigma-Aldrich) for 1 h at room temperature and embedded using FluorSave (Merck Millipore). Images were taken using a Leica confocal microscope.

Conventional immunohistochemistry staining in human tissues. Immunohistochemical staining on human colorectal adenoma and colorectal cancer tissue sections was carried out using an MaxVision<sup>TM</sup> kit (MXB Biotech, Fujian, China) according to the manufacturer's recommendation. Serial slides of de-paraffinized tissue sections were labeled with rabbit polyclonal antibodies against human H3K79me2 (Abcam, ab177184). Nuclear H3K79me2 was scored using the immunoreactive score (IRS) as a method of assessing the extent of nuclear

immunoreactivity. The IRS takes into account the percentage of positive cells (1–4 score for 0–25%, 25–50%, 50–75%, and 75–100%, respectively) in each intensity category (0–3) and computes a final score, on a continuous scale between 0 and 12.

Immunofluorescence staining in human tissues.<sup>23,24</sup> Human colorectal adenoma and colorectal cancer tissues were de-paraffinized. The staining was performed with PerkinElmer's Opal<sup>TM</sup> multiplexed reagents according to the manufacturer's instructions: Opal 520, Opal 570, and Opal 650.<sup>23,24</sup> Multiple antigen retrieval steps using either AR6 (CD3) or AR9 (Foxp3, ROR $\gamma$ t, and DAPI) antigen retrieval buffer was used for the removal of primary and secondary antibodies. The following primary and secondary antibodies were used: rabbit anti-human/mouse FOXP3 (Clone: D6O8R, Cell Signaling), rabbit polyclonal antibody against CD3 (DAKO), anti-ROR $\gamma$ t antibody (Clone: EPR20006, Abcam), immPRESS<sup>TM</sup> HRP Goat anti-rabbit (Vector), and immPRESS<sup>TM</sup> HRP Horse anti-mouse IgG (Vector). Tissue slides were scanned on the Mantra Automated Quantitative Pathology Imaging System and analyzed using Inform software (Perkin-Elmer). At least 3 fields were acquired across the entire tissue sections and analyzed for FOXP3, ROR $\gamma$ t, and CD3 expression. Any discrepancies were resolved by subsequent consultation with a diagnostic pathologist.

### Statistical analysis

Statistical analysis was performed in GraphPad Prism statistical software (version 6). P values were calculated using T test, Mann-Whitney U-test, Spearman's correlation test,  $\chi^2$  test, or one-way ANOVA as indicated. P value < .05 was considered statistically significant.

## Results

### IEC-Dot1l supports colorectal tumorigenesis

DOT1L is involved in the regulation of cancer stemness in the *in vitro* cultured human colorectal cancer cell lines.<sup>14</sup> We wondered if DOT1L directly affects intestinal tumorigenesis. To address this in an *in vivo* model, we generated intestinal epithelial cell (IEC)-specific *Dot1l*-deficient (*Dot1l* <sup>$\Delta$ IEC</sup>) mice by crossing mice carrying a floxed allele of *Dot1l* (*Dot1l*<sup>FF</sup>)<sup>12</sup> to *Villin*-cre mice.<sup>20</sup> *Dot1l* <sup>$\Delta$ IEC</sup> mice were born at normal Mendelian frequencies (Supplementary Figure 1a). We isolated and sorted epithelial cell adhesion molecule (EpcAM)<sup>+</sup> IECs (Supplementary Figure 1b) from colon of these mice. Real-time PCR (Supplementary Figure 1c) and Western blotting (Supplementary Figure 1d) confirmed IEC-specific *Dot1l* deletion. We observed no apparent alterations in intestinal morphology in *Dot1l* <sup>$\Delta$ IEC</sup> mice (Supplementary Figure 1e).

To investigate the potential role of epithelium-intrinsic *Dot1l* function in intestinal tumorigenesis, we established two different mouse intestinal tumor models. We generated *Dot1l* <sup>$\Delta$ IEC</sup>*Apc*<sup>Min</sup> (*Apc*<sup>Min</sup> $\Delta$ IEC) mice by breeding *Dot1l* <sup>$\Delta$ IEC</sup> mice with *Apc*<sup>Min</sup> mice and challenged these mice with DSS to promote colorectal cancer development. We observed low tumor numbers (Figure 1a–b) and small tumor load (Figure 1c) in *Dot1l* <sup>$\Delta$ IEC</sup>*Apc*<sup>Min</sup> mice as compared to *Dot1l*<sup>fl/fl</sup>

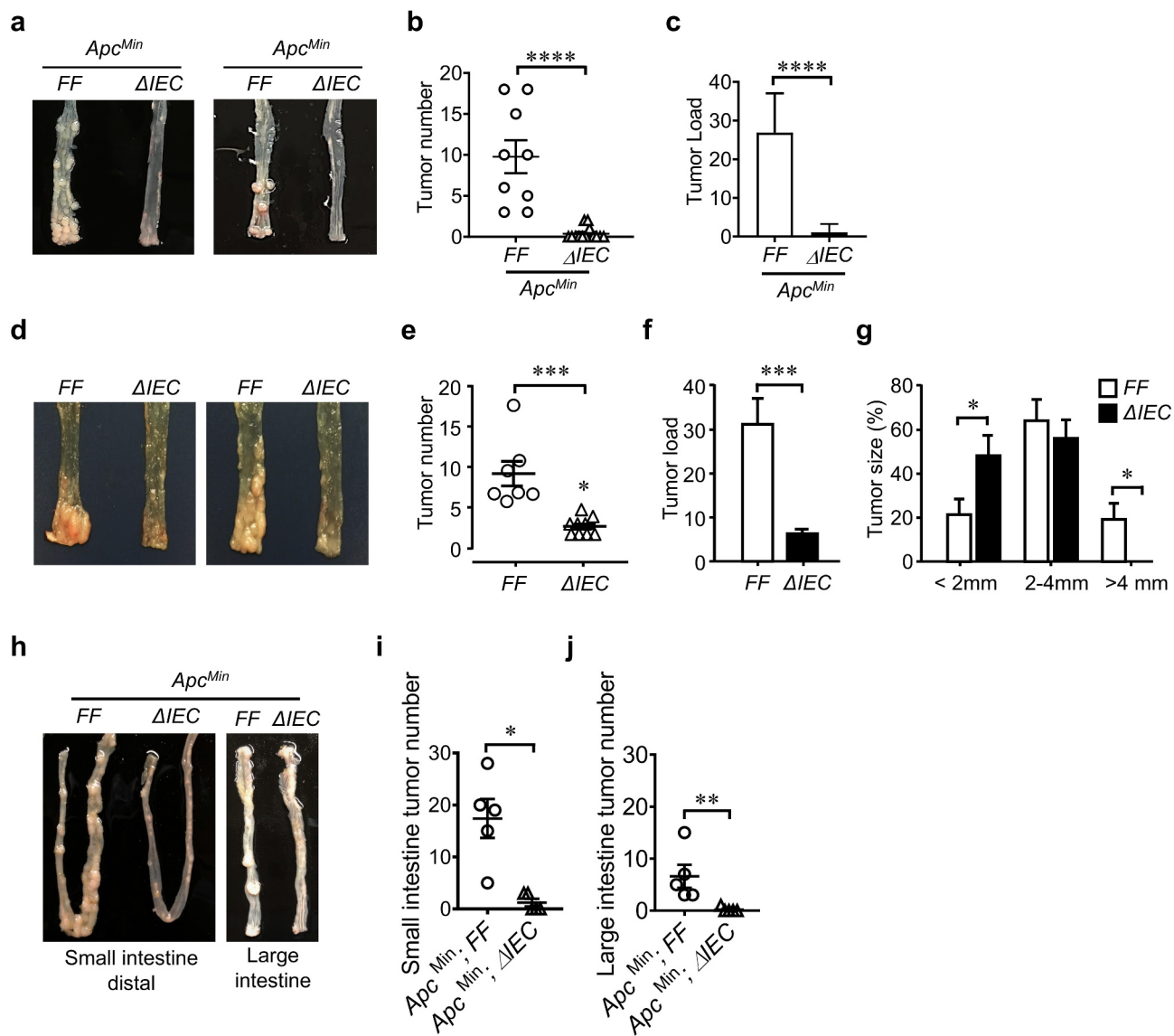


**Figure 1.** IEC-*Dot1l* supports colorectal tumorigenesis. (a) Macroscopic view of the representative colons from *Apc<sup>Min</sup>Dot1<sup>FF</sup>* or *Apc<sup>Min</sup>Dot1<sup>ΔIEC</sup>* mice on day 30 in the DSS induced tumor model. (b and c) Colorectal tumor numbers (b) and loads (c) are quantified in *Apc<sup>Min</sup>Dot1<sup>FF</sup>* (n = 9) or *Apc<sup>Min</sup>Dot1<sup>ΔIEC</sup>* (n = 13) mice on day 30 in the DSS induced tumor model. \*\*\*\*P < .0001, Mann-Whitney U-test for tumor number, \*\*\*\*P < .0001, Student's t-test for tumor load. (d) Macroscopic view of the representative mouse colon from *Dot1<sup>FF</sup>* or *Dot1<sup>ΔIEC</sup>* mice on day 70 in the cancer model. (e and f) Colorectal cancer numbers (e) and tumor loads (f) are quantified in *Dot1<sup>FF</sup>* (n = 7) and *Dot1<sup>ΔIEC</sup>* (n = 9) mice on day 70 of the cancer model. \*\*\*P = .001, Mann-Whitney U-test for tumor number, \*\*\*P = .0002, Student's t-test for tumor load. (g) Tumor size distribution is shown in *Dot1<sup>FF</sup>* and *Dot1<sup>ΔIEC</sup>* mice. P = .0408 (tumor < 2 mm), \*P < .05, Chi-squared test. (h) Macroscopic view of the representative mouse distal small (left) and large (right) intestines in *Apc<sup>Min</sup>Dot1<sup>FF</sup>* or *Apc<sup>Min</sup>Dot1<sup>ΔIEC</sup>* mice on day 210 in the spontaneous tumor model. (i and j) Tumor numbers were counted in small (i) and large intestines in *Apc<sup>Min</sup>Dot1<sup>FF</sup>* and *Apc<sup>Min</sup>Dot1<sup>ΔIEC</sup>* mice on day 210 of spontaneous tumor model. \*P = .0109 for small intestine, \*\*\*P = .0095 for large intestine, Mann-Whitney U-test.

*flApc<sup>Min</sup>* (*Apc<sup>Min</sup>FF*) mice. The data suggests that epithelium intrinsic *Dot1l* plays a role in colorectal carcinogenesis. In addition, we established an AOM/DSS-induced colorectal cancer model in *Dot1<sup>FF</sup>* and *Dot1<sup>ΔIEC</sup>* mice. Again, we found that tumor numbers (Figure 1d–e), tumor load (Figure 1f), and larger tumors (>4 mm) (Figure 1g) were reduced in *Dot1<sup>ΔIEC</sup>* mice, as compared to control littermates. Furthermore, to explore a role of *Dot1l* in spontaneous intestinal tumor development, we maintained *Dot1<sup>FF</sup>Apc<sup>Min</sup>* and *Dot1<sup>ΔIEC</sup>Apc<sup>Min</sup>* mice for 6–7 months in the absence of DSS and AOM administration. We found less tumors in small and large intestines in *Dot1<sup>ΔIEC</sup>Apc<sup>Min</sup>* mice than *Dot1<sup>FF</sup>Apc<sup>Min</sup>* mice (Figure 1h, i and j). Together, the results reveal a pro-tumor role of intrinsic intestinal epithelium *Dot1l* in colorectal tumorigenesis.

### Intestinal *Dot1l* affects IEC proliferation

Cancer cell proliferation contributes to cancer phenotype and progression. We wondered if intrinsic intestinal epithelium *Dot1l* affects colorectal cancer cell proliferation. We performed hematoxylin and eosin (H & E) staining in intestinal tissues and observed no histological difference between *Dot1<sup>FF</sup>* and *Dot1<sup>ΔIEC</sup>* mice (Supplementary Figure 2a). Mice were treated with BrdU. We detected similar levels of BrdU<sup>+</sup> intestinal epithelial cells between *Dot1<sup>FF</sup>* and *Dot1<sup>ΔIEC</sup>* mice (Supplementary Figure 2b and c). The data suggest that genetic deficiency of *Dot1l* does not affect intestinal epithelial cells in homeostasis. Interestingly, we observed tubular colorectal adenomas with high-grade dysplasia in *Dot1<sup>FF</sup>* mice and low-

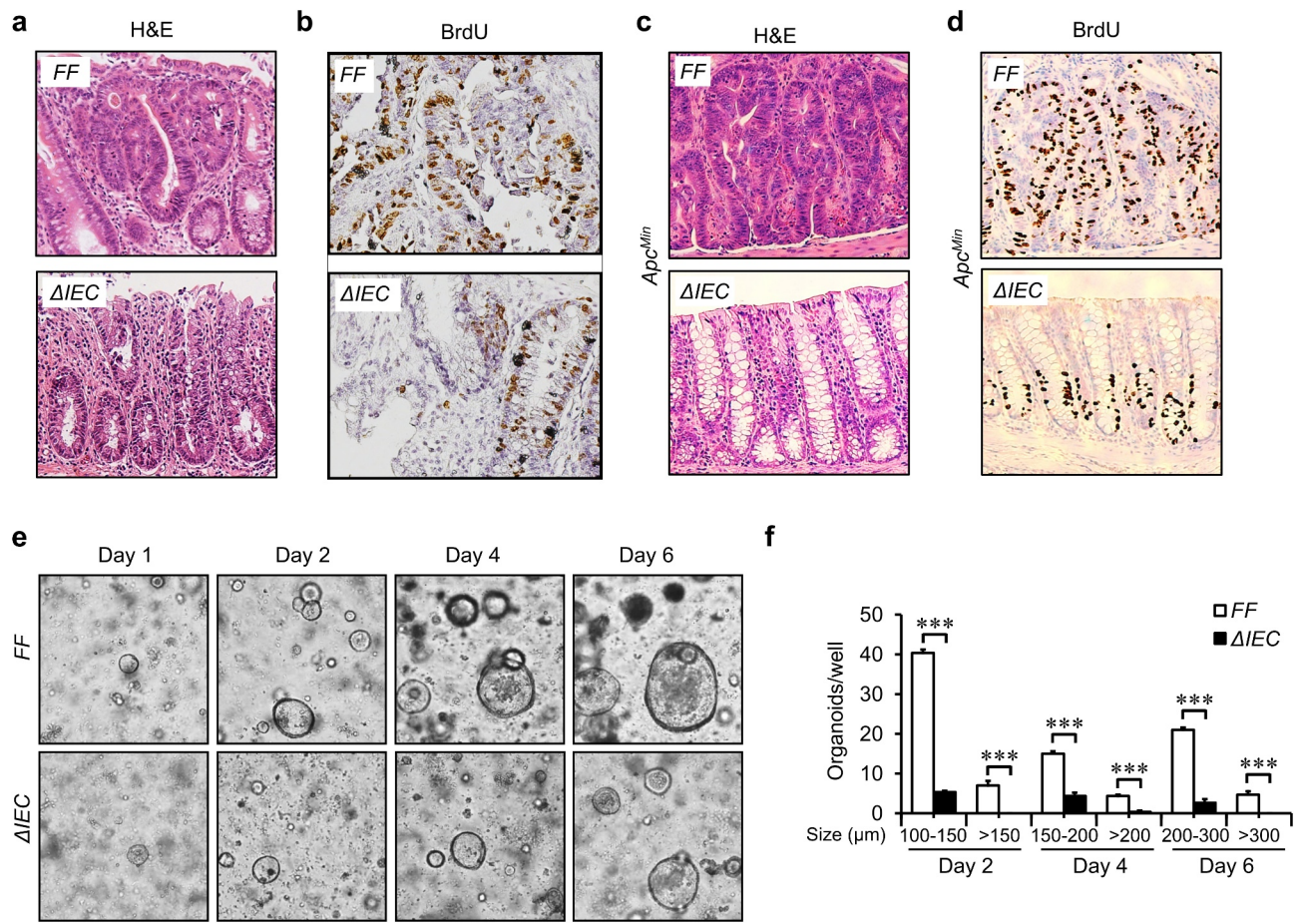


**Figure 2.** Intestinal *Dot1l* affects IEC proliferation. (a and b) Representative Hematoxylin and eosin (H & E) histology (a) and BrdU histology (b) of colorectal from *Dot1l<sup>FF</sup>* and *Dot1l<sup>ΔIEC</sup>* mice on day 70 of the colorectal cancer model. One of 5 is shown. (c and d) Representative H&E histology (c) and BrdU histology (d) of mouse colorectals from *Apc<sup>Min</sup>Dot1l<sup>FF</sup>* and *Apc<sup>Min</sup>Dot1l<sup>ΔIEC</sup>* mice on day 30 of the DSS induced colorectal cancer model. One of 5 is shown. (e) Representative images of tumor organoids from *Dot1l<sup>FF</sup>* and *Dot1l<sup>ΔIEC</sup>* mice on day 70 of the colorectal cancer model. Scale bar, 75 μm. Data represents one of three independent experiments. (f) Tumor organoid numbers and sizes are shown in *Dot1l<sup>FF</sup>* and *Dot1l<sup>ΔIEC</sup>* mice on day 70 of the colorectal cancer model. n = 3, \*\*\*P < .001 for all groups in different sizes of tumor organoids, Student's t-test.

grade dysplasia in *Dot1l<sup>ΔIEC</sup>* mice in AOM-DSS induced intestinal tumor model (Figure 2a). Furthermore, we detected less BrdU<sup>+</sup> proliferative cells in *Dot1l<sup>ΔIEC</sup>* mice than *Dot1l<sup>FF</sup>* mice (Figure 2b and Supplementary Figure 2d). In line with this, we observed high-grade dysplasia (Figure 2c) and high levels of BrdU<sup>+</sup> proliferative cells (Figure 2d and Supplementary Figure 2e) in *Dot1l<sup>FF</sup>Apc<sup>Min</sup>* mice as compared with *Dot1l<sup>ΔIEC</sup>Apc<sup>Min</sup>* mice. We conducted intestinal tumor organoid culture assay. We found that the growth and the size of tumor organoids were reduced in *Dot1l<sup>ΔIEC</sup>* mice compared to *Dot1l<sup>FF</sup>* mice (Figure 2e–f). In addition, treatment of *Dot1l<sup>FF</sup>Apc<sup>Min</sup>* tumor-derived organoids with a DOT1L methyltransferase specific inhibitor, EPZ004777<sup>25</sup> can also reduce organoids growth (Supplementary Figure 2 f and g). Thus, epithelium intrinsic *Dot1l* supports tumor cell proliferation.

### Intestinal *Dot1l* affects the Wnt/β-catenin pathway

We next explored molecular targets of DOT1L in promoting tumorigenesis and tumor cell proliferation. The Wnt/β-catenin signaling pathway is involved in colorectal carcinogenesis.<sup>6,7,26</sup> Mutations in exon 3 of the β-catenin gene was also found in

AOM/DSS induced mouse colorectal tumors.<sup>27</sup> We examined whether *Dot1l* mediated methylation of H3K79me2 affected canonical Wnt/β-catenin signaling pathway in vivo. Expression levels of *Sox4*, a typical Wnt/β-catenin target gene, were comparable in naïve *Dot1l<sup>FF</sup>* and *Dot1l<sup>ΔIEC</sup>* colon epithelial cells (Supplementary Figure 3a). Interestingly, real-time PCR (Figure 3a) and Western blotting (Figure 3b) demonstrated higher expression levels of canonical Wnt target genes, such as *Axin2*, *Sox4*, *Ephb3*, and *Lgr5* in *Dot1l<sup>FF</sup>* tumors than in *Dot1l<sup>ΔIEC</sup>* tumor in the AOM/DSS induced tumor. In line with this, immunofluorescence staining showed higher levels of β-catenin and *Axin2* in early-stage colorectal cancer epithelial cells in *Dot1l<sup>FF</sup>* mice than *Dot1l<sup>ΔIEC</sup>* mice in the AOM/DSS model (Figure 3c). *Axin2* is a canonical Wnt target gene.<sup>6,7</sup> The result indicates a higher Wnt/β-catenin signaling in *Dot1l<sup>FF</sup>* mice than *Dot1l<sup>ΔIEC</sup>* mice.

Human colorectal cancer cell lines DLD-1 and HT29 have increased β-catenin-regulated gene transcription.<sup>28</sup> To determine whether DOT1L regulated the Wnt target genes in human colorectal cancer cells, we treated human colorectal cancer cells with EPZ004777. EPZ004777 treatment inhibited H3K79 methylation in DLD-1 and HT29 cells (Supplementary Figure 3b). Accordingly, EPZ004777 suppressed the expression

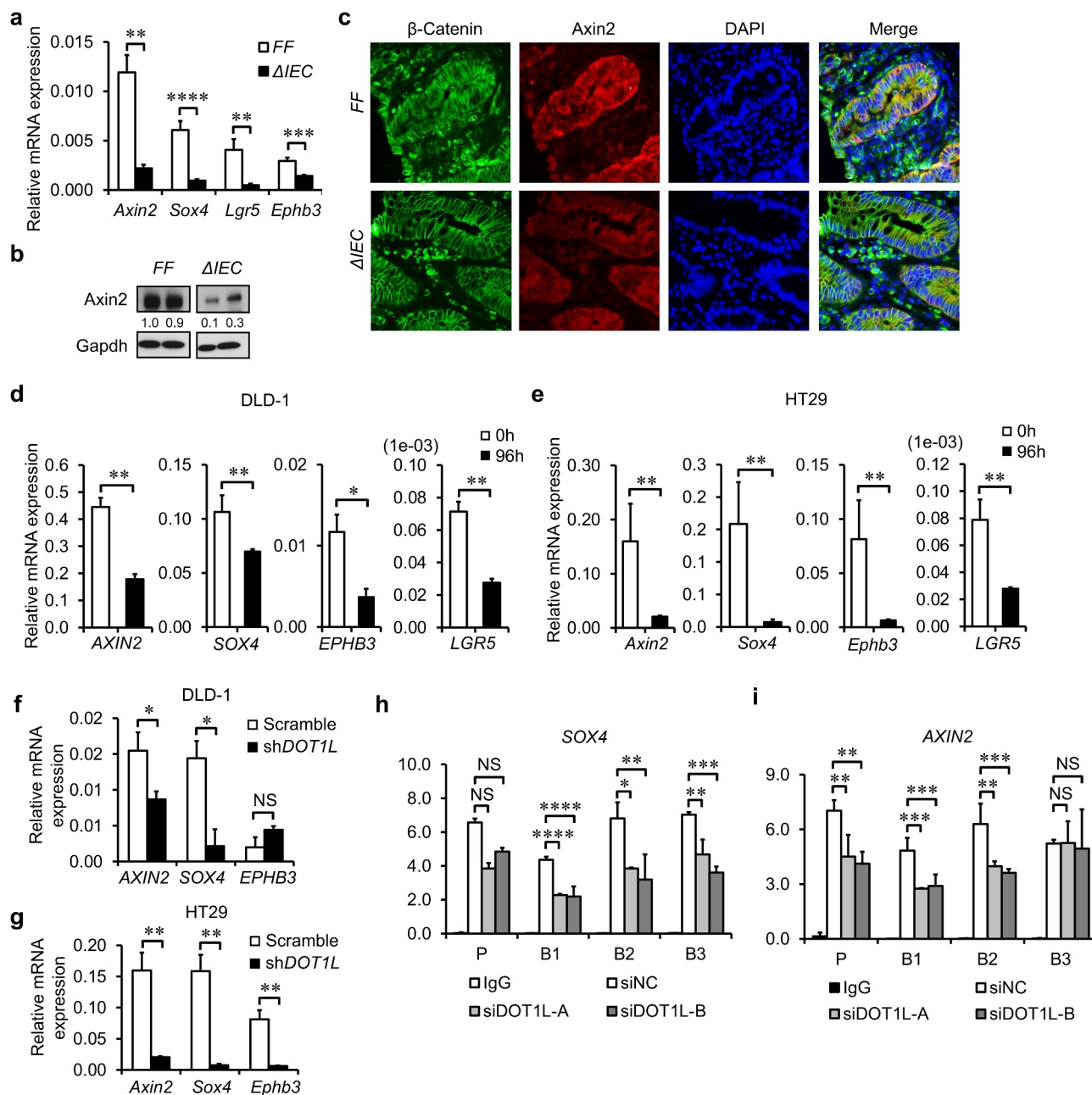


**Figure 3.** Intestinal *Dot1l* affects the Wnt/ $\beta$ -catenin pathway. (a) Wnt/ $\beta$ -catenin downstream genes mRNA expression from *Dot1l*<sup>FF</sup> and *Dot1l* <sup>$\Delta$ IEC</sup> mice day 70 of the colorectal cancer model,  $n = 7-8$ ,  $**P = .0069$  for *Axin2*,  $****P < .0001$  for *Sox4*,  $**P = .0038$  for *Lgr5*,  $***P = .0006$  for *Ephb3*, Student's t-test. (b) Western blot of Axin2 expression from *Dot1l*<sup>FF</sup> and *Dot1l* <sup>$\Delta$ IEC</sup> mice day 70 of the colorectal cancer model. One of three is shown. (c) Immunofluorescence staining of  $\beta$ -catenin and Axin2 in *Dot1l*<sup>FF</sup> and *Dot1l* <sup>$\Delta$ IEC</sup> colorectal on day 14 of AOM-DSS model. Green:  $\beta$ -catenin, Red: Axin2, Blue: DAPI. (d and e) Effect of EPZ004777 on Wnt/ $\beta$ -catenin downstream gene mRNA expression in DLD-1 (d) and HT29 (e) cells. (d)  $**P = .0023$  for *AXIN2*,  $**P = .0026$  for *SOX4*,  $*P = .0475$  for *EPHB3*,  $**P = .0026$  for *LGR5*. (e)  $**P = .0081$  for *AXIN2*,  $**P = .0046$  for *SOX4*,  $**P = .007$  for *EPHB3*. Student's t-test. (f and g) Effect of *DOT1L* knockdown on Wnt/ $\beta$ -catenin downstream gene mRNA expression in DLD-1 (f) and HT29 (g) cells. (f)  $*P < .05$ . (g)  $**P = .0081$  for *AXIN2*,  $**P = .0046$  for *SOX4*,  $**P = .007$  for *EPHB3*, Student's t-test. (h and i) H3K79me2 ChIP on the promoter (p) and different gene body regions (B1, B2, and B3) of *SOX4* (h) and *AXIN2* (i) in DLD-1 cells. NS,  $P > .05$ ,  $*P \leq .05$ ,  $**P \leq .01$ ,  $***P \leq .001$ ,  $****P \leq .0001$ , one-way ANOVA.

of *AXIN2*, *SOX4*, *EPHB3*, and *LGR5* in DLD-1 (Figure 3d) and HT29 (Figure 3e) cells. Genetic knock down of *DOT1L* with specific shRNAs caused reduced expression of *AXIN2*, and *SOX4* in DLD-1 (Figure 3f) and HT29 cells (Figure 3g) and reduced *EPHB3* in HT29 cells (Figure 3g). *DOT1L* can bound to both promoter<sup>29</sup> and gene body<sup>30</sup> of actively transcribed genes. Chromatin immunoprecipitation (ChIP)-seq matrix from ENCODE showed H3K79me2 occupation in the promoter and gene body regions of *SOX4* and *AXIN2* (Supplementary Figure 3c and d). We used ChIP assay to evaluate the

occupancy of H3K79me2 at the promoter and gene body regions of *SOX4* and *AXIN2* in DLD-1 cells (Supplementary Figure 3e and f). We found that H3K79me2 was enriched in both *SOX4* and *AXIN2* loci. Knockdown *DOT1L* resulted in reduced H3K79me2 level in the gene body region of *SOX4* loci (Figure 3h). While knockdown *DOT1L* caused the reduction of H3K79me2 level at both promoter region and early gene body regions of *AXIN2* loci (Figure 3i). These results suggest that *DOT1L* targets the Wnt/ $\beta$ -catenin signaling gene transcription via H3K79me2.

### Intestinal *Dot1l* alters immune cell subsets

In addition to activation of the Wnt/ $\beta$ -catenin pathway, chronic inflammation is a risk factor in colorectal carcinogenesis.<sup>17</sup> Activation of WNT/ $\beta$ -catenin signaling also has been linked with immune escape and T cell exclusion.<sup>31</sup> In support of this notion, in the AOM-DSS mode, *Dot1l* <sup>$\Delta$ IEC</sup> mice exhibited higher body weight (Figure 4a), longer colon length (Supplementary Figure 4a), and reduced disease score (Supplementary Figure 4b) as compared to their *Dot1l*<sup>FF</sup> littermates. This suggests that DOT1L may facilitate intestinal inflammation, thereby affecting tumorigenesis. As local immune cell activation contributes to inflammation, we compared immune cell subsets in lamina propria in the intestinal microenvironment in *Dot1l*<sup>FF</sup> and *Dot1l* <sup>$\Delta$ IEC</sup> mice. We detected a decrease in IL-17<sup>+</sup>CD4<sup>+</sup> T (Th17) and IL-22<sup>+</sup>CD4<sup>+</sup> T (Th22) cells in colorectal tissues in *Dot1l* <sup>$\Delta$ IEC</sup> mice as compared to *Dot1l*<sup>FF</sup> littermates (Figure 4b–c). This was not observed in mesenteric lymph nodes (mLNs) (Supplementary Figure 4c). Accordingly, the levels of several pro-inflammatory gene transcripts, including *Cox2*, *Il1b*, and *Il23a*, were lower in *Dot1l* <sup>$\Delta$ IEC</sup> tumor tissues than those in *Dot1l*<sup>FF</sup> colorectal tissues (Supplementary Figure 4d). These pro-inflammatory molecules might be from myeloid cells<sup>32</sup> and can induce Th17 and Th22 cells.<sup>33–35</sup> Hence, *Dot1l* supports inflammatory immune cells, including Th17 and Th22 cells, in colorectal cancer. It has been reported that there is a balance between Th17 cells and Treg cells in gut.<sup>33,36,37</sup> Gut-specific ROR $\gamma$ t<sup>+</sup>Foxp3<sup>+</sup> Treg cells are highly suppressive and protect chronic intestinal inflammation.<sup>38–40</sup> The percentage of lamina propria

Foxp3<sup>+</sup>CD4<sup>+</sup> Tregs and ROR $\gamma$ t<sup>+</sup>Foxp3<sup>+</sup> Tregs were comparable in *Dot1l*<sup>FF</sup> and *Dot1l* <sup>$\Delta$ IEC</sup> mice in homeostasis condition (Supplementary Figure 4e and f). However, we found that the percentage of tumor infiltrating Foxp3<sup>+</sup>CD4<sup>+</sup> Treg cells, particularly ROR $\gamma$ t<sup>+</sup>Foxp3<sup>+</sup> Treg cells were increased in *Dot1l* <sup>$\Delta$ IEC</sup> mice as compared to *Dot1l*<sup>FF</sup> mice *Dot1l*<sup>FF</sup> in the AOM-DSS model (Figure 4d–e) and *Apc*<sup>Min</sup> model (Figure 4f–g). The difference of ROR $\gamma$ t<sup>+</sup>Foxp3<sup>+</sup> Tregs was not observed in mesenteric lymph nodes (Figure 4f–g). Altogether, the data suggest *Dot1l* in IECs affects intestinal T cell subsets, thereby altering colorectal inflammation.

### H3K79 methylation status correlates with ROR $\gamma$ <sup>+</sup> Tregs in human colorectal cancer

Given the interplay between intestinal *Dot1l* and lamina propria immune cell subsets, and its potential link to colorectal carcinogenesis in mouse models, we extended our studies to patients with colorectal adenoma and early colorectal cancer. To this end, we detected H3K79 di-methylation with immunohistochemistry in human colorectal adenoma and early colorectal cancer tissues (Figure 5a). The levels of H3K79me2 expression were lower in colorectal adenoma than colorectal cancer (Figure 5a–b). Based on mouse data (Figure 4f–g), we assumed that there might exist a correlation between H3K79 methylation level and ROR $\gamma$ <sup>+</sup>FOXP3<sup>+</sup> Treg cells in patients with colorectal adenoma and early carcinoma. To this end, we conducted multiple color immunofluorescence tissue staining in human colorectal adenoma and early carcinoma tissues

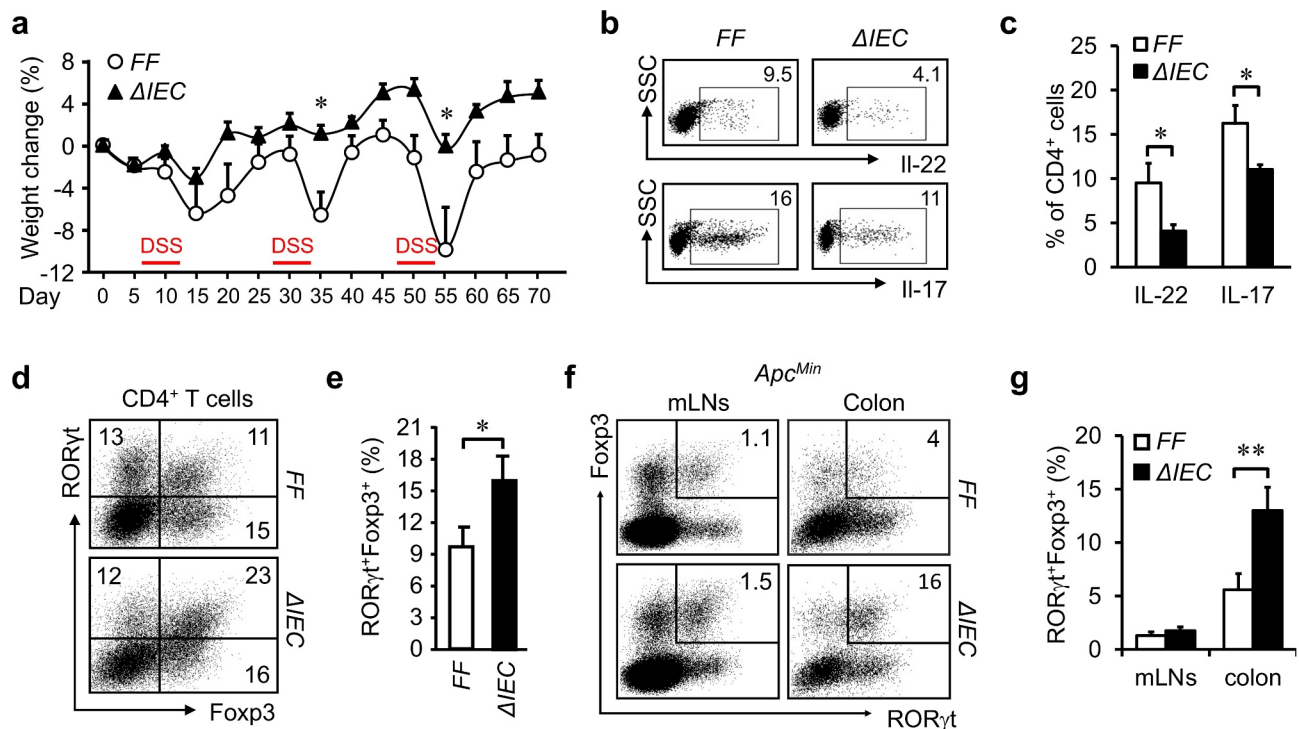


**Figure 4.** Intestinal *Dot1l* alters T cell subsets. (a) Body weight changes at the indicated time points in the AOM-DSS induced cancer model. DSS water treated windows are highlighted. *Dot1l*<sup>FF</sup> (n = 7), *Dot1l* <sup>$\Delta$ IEC</sup> (n = 8), \**P* = .0253 (Day 35), \**P* = .0266 (Day 55), 2way ANOVA. (b, c) Flow cytometry analysis shows IL-22 and IL-17 expressing CD4<sup>+</sup> T cells in lamina propria in colorectal cancer model. n = 6/group, \**P* = .04 for IL-17; \**P* = .05 for IL-22, Student's *t*-test. (d, e) Dot plots show ROR $\gamma$ t<sup>+</sup> Foxp3<sup>+</sup> CD4<sup>+</sup> T cell subsets in lamina propria in *Dot1l*<sup>FF</sup> and *Dot1l* <sup>$\Delta$ IEC</sup> mice on day 70 of the colorectal cancer model. Mean  $\pm$  SEM, n = 7. \**P* = .05, Student's *t*-test. (f, g) Dot plots show ROR $\gamma$ t<sup>+</sup> Foxp3<sup>+</sup>CD4<sup>+</sup> T cell subsets in mesenteric lymph nodes (mLNs) and colon tumor tissues in *Apc*<sup>Min</sup>*Dot1l*<sup>FF</sup> and *Apc*<sup>Min</sup>*Dot1l* <sup>$\Delta$ IEC</sup> mice on day 210 of spontaneous tumor model. n = 5–6. \*\*\**P* = .009, Student's *t*-test.

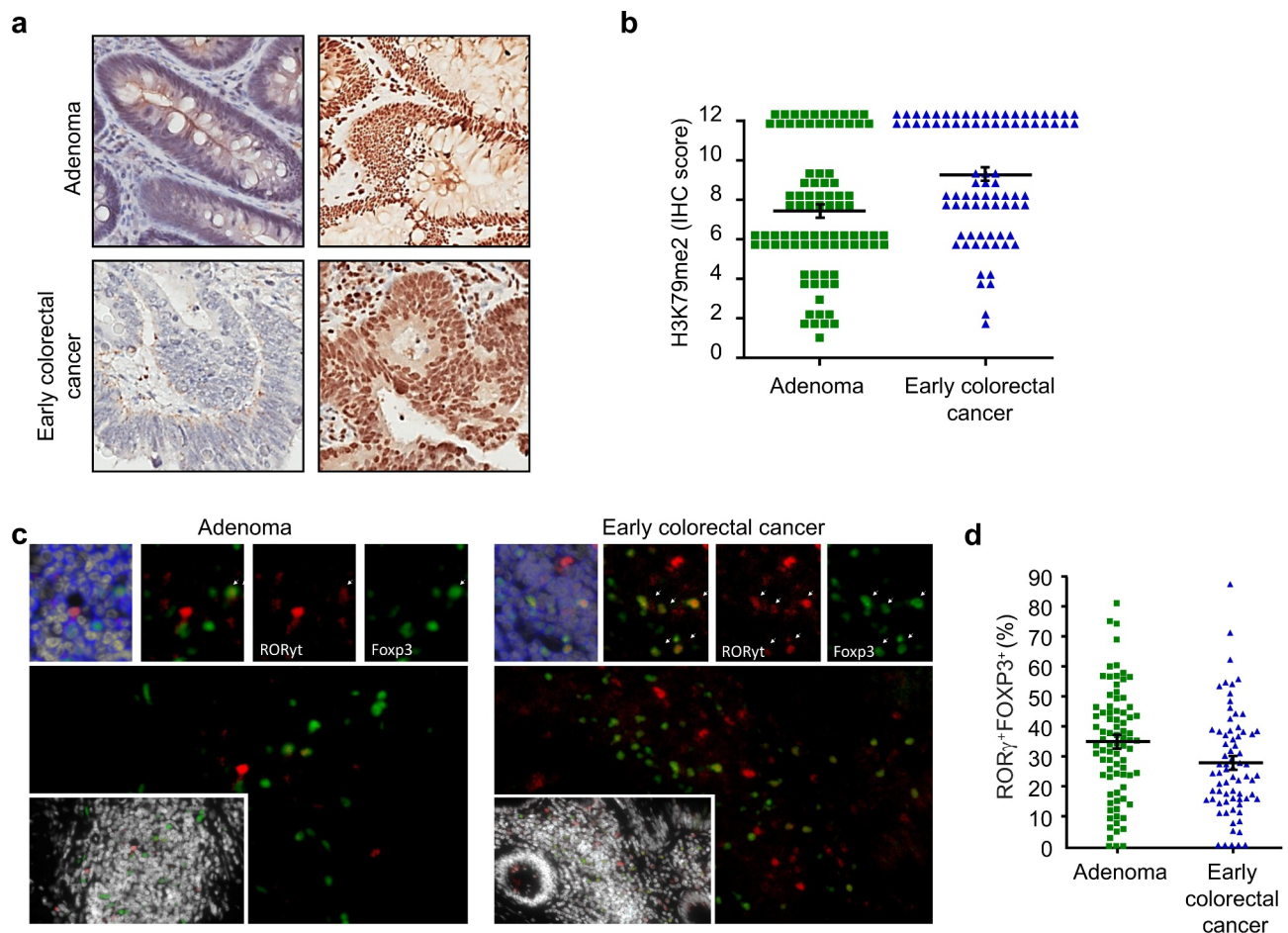


**Figure 5.** H3K79 methylation status correlates with ROR $\gamma^+$  Tregs in human colorectal cancer. (a and b) H3K79me2 immunohistochemistry staining in human colorectal adenoma and early colorectal cancer tissues. (a) 4 representative images showed different levels of H3K79me2 expression. 40X magnifications. (b) Quantification of H3K79me2 levels from 5a in colorectal adenoma (green) and early carcinoma (blue) patients. Colorectal adenoma,  $n = 87$ ; early colorectal cancer,  $n = 82$ ,  $***P = .00018$ , Mann-Whitney  $U$ -test. (c and d) ROR $\gamma^+$ FOXP3 $^+$  T cell staining in human colorectal adenoma and early colorectal cancer tissues. (c) Human colorectal adenoma tissues (left) and early colorectal tissues (right) were stained for CD3 (blue), FOXP3 (green), ROR $\gamma$ t (red), and DAPI (white). One representative image is shown. 40X magnifications. (d) ROR $\gamma^+$ FOXP3 $^+$  T cells were quantified and compared in colorectal adenoma (green) and early carcinoma (blue) patients. Colorectal adenoma,  $n = 82$ ; early colorectal cancer,  $n = 72$ ,  $**P = .009$ , Mann-Whitney  $U$ -test.

to identify and quantify ROR $\gamma^+$ FOXP3 $^+$  Treg cells (Figure 5c). We detected high ROR $\gamma^+$ FOXP3 $^+$  T cells in human colorectal adenoma and colorectal cancer tissues. There were more ROR $\gamma^+$ FOXP3 $^+$  T cells in colorectal adenoma than early colorectal cancer tissues (Figure 5d). Thus, there is a link between H3K79 methylation level and ROR $\gamma^+$ FOXP3 $^+$  Tregs in the gut during colorectal cancer development.

## Discussion

Chronic immune stimulation and the Wnt/ $\beta$ -catenin pathway activation are two critical contributors to colorectal carcinogenesis. Our current work demonstrates that intestinal epithelial cell methyltransferase *DOT1L* is an intrinsic mechanism connecting these 2 factors in colorectal cancer.

*DOT1L* mediates H3K79 methylation.<sup>10</sup> We have previously studied how Th22 cells affect cancer stemness via the *DOT1L* and H3K79me2 axis in the human colorectal cancer microenvironment.<sup>14</sup> Using intestinal epithelium-specific *Dot1l* knockout mice, we have demonstrated a pro-tumor role of *Dot1l* in the *Apc*<sup>Min</sup> and AOM/DSS-induced colorectal tumor models. Furthermore, we have observed an increase in H3K79me2 levels

from colorectal adenoma to carcinoma in humans. The data reveal that intestinal epithelial intrinsic *DOT1L* directly affects colorectal carcinogenesis. Given that colorectal cancer development is associated with chronic inflammation and oncogenic pathway activation, we hypothesized that *DOT1L* contributes to colorectal carcinogenesis via altering both chronic immune activation and oncogenic gene pathway activation in the intestinal microenvironment. In support of this, we observed a decrease in Th17 and Th22 cells, and an increase in ROR $\gamma^+$ Foxp3 $^+$  regulatory T cells in lamina propria in *Dot1l* <sup>$\Delta$ IEC</sup> mice. In line with mouse data, high levels of Th17 and Th22 cells are detected in patients with colorectal cancer and chronic bowel diseases,<sup>33</sup> and ROR $\gamma^+$ Foxp3 $^+$  T cells negatively correlated with colorectal tumor stage and H3K79me2 level in patients with colorectal cancer. Thus, it seems that elevated *DOT1L* may tilt the balance between inflammatory and regulatory T cell subsets in the gut, thereby supporting and maintaining a chronic immune active microenvironment. In line with this possibility, loss of ROR $\gamma^+$ Foxp3 $^+$  T cells can lead to an increase in Th17 cells and exacerbated 2,4,6-trinitrobenzene sulfonic acid (TNBS)-induced colitis in mice.<sup>38</sup> Thus, *DOT1L* mediated-H3K79 methylation correlates with chronic immune activation and colorectal cancer progression.



In addition to chronic immune activation, we have found a close relationship between DOT1L and the Wnt/ $\beta$ -catenin signaling pathway. We have detected reduced levels of several downstream genes in the Wnt/ $\beta$ -catenin signaling pathway in *Dot1l*<sup>ΔIEC</sup> mice. Accordingly, *Dot1l*<sup>ΔIEC</sup> intestinal epithelium cells form less organoids ex vivo compared to wild type cells. These results are supported and validated in human colorectal cancer cells with genetic and biochemical manipulation of DOT1L. Furthermore, ChIP-seq and ChIP-PCR assay reveal high levels of H3K79me2 signals in the promoters of the Wnt/ $\beta$ -catenin target genes in colorectal cancer cells. Thus, DOT1L mediated-H3K79 methylation can regulate the Wnt/ $\beta$ -catenin signaling pathway, thereby impacting colorectal cancer progression.

In summary, DOT1L, as an intrinsic molecular node, orchestrates two key elements, chronic inflammation and oncogenic pathway activation, to promote colorectal cancer development. Apart from patients with mixed-lineage leukemia,<sup>12,41</sup> the current study provides a rationale for initiating small-molecule screening to target DOT1L activity in patients at high risk of and/or with colorectal cancer.

## Acknowledgments

We thank Drs. Jixuan Han, Yuanhong Xie, Ming Zhong, Sanjun Cai, Guoxiang Cai, Zhanju Liu and Xiaomin Sun for collecting clinical samples and information for this work. We are grateful for Dr. Jay Hess for providing *Dot1l* fl/fl mice, Dr. Deborah L. Gumucio for *Villin*-Cre mice, and Kwi Kim for technical assistance.

## Author contributions

Conceptualization, D.S.; E.R.F.; J.Y.F.; W.Z.; Methodology, D.S., W.W.; F.G.; M.P.; W.D.; S.W.; S.G.; L.V.; Y.C.; Investigation, D.S., W.W.; F.G.; W.D.; S.W.; L.V.; Y.C. I.K.; Writing-Original Draft, D.S.; W.W.; W.Z.; Writing-Reviewing & editing, D.S., W.W.; F.G.; E.R.F.; I.K.; J.Y.F.; W.Z.; Funding Acquisition, W.Z.; Supervision, I.K.; J.Y.F.; W.Z.

## Disclosure statement

No potential conflict of interest was reported by the author(s).

## Funding

This work was supported by the University of Michigan endowment.

## References

- Le DT, Uram JN, Wang H, Bartlett BR, Kemberling H, Eyring AD, Skora AD, Lubner BS, Azad NS, Laheru D, et al. PD-1 blockade in tumors with mismatch-repair deficiency. *N Engl J Med*. 2015 Jun;372(26):2509–2520. doi:10.1056/NEJMoa1500596.
- Le DT, Durham JN, Smith KN, Wang H, Bartlett BR, Aulakh LK, Lu S, Kemberling H, Wilt C, Lubner BS, et al. Mismatch repair deficiency predicts response of solid tumors to PD-1 blockade. *Science*. 2017 07;357(6349):409–413. doi:10.1126/science.aan6733
- Fearon ER, Vogelstein B. A genetic model for colorectal tumorigenesis. *Cell*. 1990 Jun;61(5):759–767. doi:10.1016/0092-8674(90)90186-i.
- Fearon ER. Molecular genetics of colorectal cancer. *Annu Rev Pathol*. 2011;6:479–507. doi:10.1146/annurev-pathol-011110-130235.
- Zhang B, Wang J, Wang X, Zhu J, Liu Q, Shi Z, Chambers MC, Zimmerman LJ, Shaddox KF, Kim S, et al. Proteogenomic characterization of human colon and rectal cancer. *Nature*. 2014 Sep 18;513(7518):382–387. doi:10.1038/nature13438.
- Markowitz SD, Bertagnoli MM. Molecular origins of cancer: molecular basis of colorectal cancer. *N Engl J Med*. 2009 Dec;361(25):2449–2460. doi:10.1056/NEJMra0804588.
- Vermeulen L, De Sousa E, Melo F, van der Heijden M, de Jong JH, Borovski T, Tuynman JB, Todaro M, Merz C, Rodermond H, et al. Wnt activity defines colon cancer stem cells and is regulated by the microenvironment. *Nat Cell Biol*. 2010 May;12(5):468–476. doi:10.1038/ncb2048.
- Hecht A, Vleminckx K, Stemmler MP, van Roy F, Kemler R. The p300/CBP acetyltransferases function as transcriptional coactivators of beta-catenin in vertebrates. *EMBO J*. 2000 Apr 17;19(8):1839–1850. doi:10.1093/emboj/19.8.1839.
- Takemaru KI, Moon RT. The transcriptional coactivator CBP interacts with beta-catenin to activate gene expression. *J Cell Biol*. 2000 Apr 17;149(2):249–254. doi:10.1083/jcb.149.2.249.
- Feng Q, Wang H, Ng HH, Erdjument-Bromage H, Tempst P, Struhl K, Zhang Y. Methylation of H3-lysine 79 is mediated by a new family of HMTases without a SET domain. *Curr Biol*. 2002 Jun 25;12(12):1052–1058. doi:10.1016/s0960-9822(02)00901-6.
- Okada Y, Feng Q, Lin Y, Jiang Q, Li Y, Coffield VM, Su L, Xu G, Zhang Y. hDOT1L links histone methylation to leukemogenesis. *Cell*. 2005 Apr 22;121(2):167–178. doi:10.1016/j.cell.2005.02.020.
- Jo SY, Granowicz EM, Maillard I, Thomas D, Hess JL. Requirement for Dot1l in murine postnatal hematopoiesis and leukemogenesis by MLL translocation. *Blood*. 2011 May 05;117(18):4759–4768. doi:10.1182/blood-2010-12-327668.
- Bian Y, Li W, Kremer DM, Sajjakulnukit P, Li S, Crespo J, Nwosu ZC, Zhang L, Czerwonka A, Pawłowska A, et al. Cancer SLC43A2 alters T cell methionine metabolism and histone methylation. *Nature*. 2020 09;585(7824):277–282. doi:10.1038/s41586-020-2682-1
- Kryczek I, Lin Y, Nagarsheth N, Peng D, Zhao L, Zhao E, Vatan L, Szeliga W, Dou Y, Owens S, et al. IL-22(+)/CD4(+) T cells promote colorectal cancer stemness via STAT3 transcription factor activation and induction of the methyltransferase DOT1L. *Immunity*. 2014 May 15;40(5):772–784. doi:10.1016/j.immuni.2014.03.010.
- Mohan M, Herz HM, Takahashi YH, Lin C, Lai KC, Zhang Y, Washburn MP, Florens L, Shilatifard A. Linking H3K79 trimethylation to Wnt signaling through a novel Dot1-containing complex (DotCom). *Genes Dev*. 2010 Mar 15;24(6):574–589. doi:10.1101/gad.1898410.
- Mahmoudi T, Boj SF, Hatzis P, Li VSW, Taouatas N, Vries RGJ, Teunissen H, Begthel H, Korving J, Mohammed S, et al. The leukemia-associated Mllt10/Af10-Dot1l are Tcf4/ $\beta$ -catenin coactivators essential for intestinal homeostasis. *PLoS Biol*. 2010 Nov 16;8(11):e1000539. doi:10.1371/journal.pbio.1000539.
- Terzić J, Grivnennikov S, Karin E, Karin M. Inflammation and colon cancer. *Gastroenterology*. 2010 Jun;138(6):2101–2114.e5. doi:10.1053/j.gastro.2010.01.058.
- Huber S, Gagliani N, Zenewicz LA, Huber FJ, Bosurgi L, Hu B, Hedl M, Zhang W, O'Connor W, Murphy AJ, et al. IL-22BP is regulated by the inflammasome and modulates tumorigenesis in the intestine. *Nature*. 2012 Nov 08;491(7423):259–263. doi:10.1038/nature11535.
- Yu T, Guo F, Yu Y, Sun T, Ma D, Han J, Qian Y, Kryczek I, Sun D, Nagarsheth N, et al. Fusobacterium nucleatum promotes chemoresistance to colorectal cancer by modulating autophagy. *Cell*. 2017 Jul 27;170(3):548–563.e16. doi:10.1016/j.cell.2017.07.008.
- Madison BB, Dunbar L, Qiao XT, Braunstein K, Braunstein E, Gumucio DL. Cis elements of the villin gene control expression in restricted domains of the vertical (crypt) and horizontal (duodenum, cecum) axes of the intestine. *J Biol Chem*. 2002 Sep 06;277(36):33275–33283. doi:10.1074/jbc.M204935200.
- Xue X, Shah YM. In vitro organoid culture of primary mouse colon tumors. *J Vis Exp*. 2013 May 75:e50210. doi:10.3791/50210.

22. Cui TX, Kryczek I, Zhao L, Zhao E, Kuick R, Roh M, Vatan L, Szeliga W, Mao Y, Thomas D, et al. Myeloid-derived suppressor cells enhance stemness of cancer cells by inducing microRNA101 and suppressing the corepressor CtBP2. *Immunity*. 2013 Sep 19;39(3):611–621. doi:10.1016/j.immuni.2013.08.025.
23. Fang M, Li Y, Huang K, Qi S, Zhang J, Zgodzinski W, Majewski M, Wallner G, Gozdz S, Macek P, et al. IL33 promotes colon cancer cell stemness via JNK activation and macrophage recruitment. *Cancer Res*. 2017 05 15;77(10):2735–2745. 10.1158/0008-5472.CAN-16-1602
24. Lin H, Wei S, Hurt EM, Green MD, Zhao L, Vatan L, Szeliga W, Herbst R, Harms PW, Fecher LA, et al. Host expression of PD-L1 determines efficacy of PD-L1 pathway blockade-mediated tumor regression. *J Clin Invest*. 2018 02 01;128(2):805–815. 10.1172/JCI96113
25. Daigle SR, Olhava EJ, Therkelsen CA, Majer C, Sneeringer C, Song J, Johnston L, Scott M, Smith J, Xiao Y, et al. Selective killing of mixed lineage leukemia cells by a potent small-molecule DOT1L inhibitor. *Cancer Cell*. 2011 Jul 12;20(1):53–65. doi:10.1016/j.ccr.2011.06.009.
26. Morin PJ, Sparks AB, Korinek V, Barker N, Clevers H, Vogelstein B, Kinzler KW. Activation of beta-catenin-Tcf signaling in colon cancer by mutations in beta-catenin or APC. *Science*. 1997 Mar;275(5307):1787–1790. doi:10.1126/science.275.5307.1787.
27. Gretten FR, Eckmann L, Gretten TF, Park JM, Li Z-W, Egan LJ, Kagnoff MF, Karin M. IKKbeta links inflammation and tumorigenesis in a mouse model of colitis-associated cancer. *Cell*. 2004 Aug 06;118(3):285–296. doi:10.1016/j.cell.2004.07.013.
28. Yang J, Zhang W, Evans PM, Chen X, He X, Liu C. Adenomatous polyposis coli (APC) differentially regulates beta-catenin phosphorylation and ubiquitination in colon cancer cells. *J Biol Chem*. 2006 Jun;281(26):17751–17757. doi:10.1074/jbc.M600831200.
29. Wu A, Zhi J, Tian T, Cihan A, Cevher MA, Liu Z, David Y, Muir TW, Roeder RG, Yu M, et al. DOT1L complex regulates transcriptional initiation in human erythroleukemic cells. *Proc Natl Acad Sci U S A*. 07 06 2021;11827. 10.1073/pnas.2106148118
30. Steger DJ, Lefterova MI, Ying L, Stonestrom AJ, Schupp M, Zhuo D, Vakoc AL, Kim J-E, Chen J, Lazar MA, et al. DOT1L/KMT4 recruitment and H3K79 methylation are ubiquitously coupled with gene transcription in mammalian cells. *Mol Cell Biol*. 2008 Apr;28(8):2825–2839. doi:10.1128/MCB.02076-07.
31. Grasso CS, Giannakis M, Wells DK, Hamada T, Mu XJ, Quist M, Nowak JA, Nishihara R, Qian ZR, Inamura K, et al. Genetic mechanisms of immune evasion in colorectal cancer. *Cancer Discov*. 2018 06;8(6):730–749. 10.1158/2159-8290.CD-17-1327
32. Kryczek I, Banerjee M, Cheng P, Vatan L, Szeliga W, Wei S, Huang E, Finlayson E, Simeone D, Welling TH, et al. Phenotype, distribution, generation, and functional and clinical relevance of Th17 cells in the human tumor environments. *Blood*. 2009 Aug 06;114(6):1141–1149. doi:10.1182/blood-2009-03-208249.
33. Zou W, Restifo NP. T(H)17 cells in tumour immunity and immunotherapy. *Nat Rev Immunol*. 2010 Apr;10(4):248–256. doi:10.1038/nri2742.
34. Zheng Y, Danilenko DM, Valdez P, Kasman I, Eastham-Anderson J, Wu J, Ouyang W. Interleukin-22, a T(H)17 cytokine, mediates IL-23-induced dermal inflammation and acanthosis. *Nature*. 2007 Feb 08;445(7128):648–651. doi:10.1038/nature05505.
35. Sano T, Huang W, Hall JA, Yang Y, Chen A, Gavzy S, Lee J-Y, Ziel JW, Miraldi E, Domingos A, et al. An IL-23R/IL-22 circuit regulates epithelial serum amyloid a to promote local effector Th17 responses. *Cell*. 2015 Oct 08;163(2):381–393. doi:10.1016/j.cell.2015.08.061.
36. Bettelli E, Carrier Y, Gao W, Korn T, Strom TB, Oukka M, Weiner HL, Kuchroo VK. Reciprocal developmental pathways for the generation of pathogenic effector TH17 and regulatory T cells. *Nature*. 2006 May;441(7090):235–238. doi:10.1038/nature04753.
37. Zou W. Regulatory T cells, tumour immunity and immunotherapy. *Nat Rev Immunol*. 2006 Apr;6(4):295–307. doi:10.1038/nri1806.
38. Sefik E, Geva-Zatorsky N, Oh S, Konnikova L, Zemmour D, McGuire AM, Burzyn D, Ortiz-Lopez A, Lobera M, Yang J, et al. Individual intestinal symbionts induce a distinct population of RORγ + regulatory T cells. *Science*. 2015 Aug;349(6251):993–997. doi:10.1126/science.aaa9420.
39. Geva-Zatorsky N, Sefik E, Kua L, Pisman L, Tan TG, Ortiz-Lopez A, Yanortsang TB, Yang L, Jupp R, Mathis D, et al. Mining the human gut microbiota for immunomodulatory organisms. *Cell*. 2017 02 23;168(5):928–943.e11. 10.1016/j.cell.2017.01.022
40. Yang BH, Hagemann S, Mamareli P, Lauer U, Hoffmann U, Beckstette M, Föhse L, Prinz I, Pezoldt J, Suerbaum S, et al. Foxp3(+) T cells expressing RORγt represent a stable regulatory T-cell effector lineage with enhanced suppressive capacity during intestinal inflammation. *Mucosal Immunol*. 2016 Mar;9(2):444–457. doi:10.1038/mi.2015.74.
41. Chang MJ, Wu H, Achille NJ, Reisenauer MR, Chou C-W, Zeleznik-Le NJ, Hemenway CS, Zhang W. Histone H3 lysine 79 methyltransferase Dot1 is required for immortalization by MLL oncogenes. *Cancer Res*. 2010 Dec 15;70(24):10234–10242. doi:10.1158/0008-5472.CAN-10-3294.